Solar Energy
And Sustainable Development
Refereed, biannual scientific journal issued by:
The Libyan Center for Solar Energy Research and Studies

# Performance Analysis of PV Solar Panels Augmented by Plane Reflectors in Elbida -Libya: An Experimental Study

**Ahmed Adel Rasheed Otman[1*], Abdul Hakim Ibrahim Awami[2], Tarek A. M. Hamad[3].**

[1,2]College of Technical Sciences Derna, Libya.
[3]Department of Sustainable and Renewable Energy Engineering, Omar Al-Mukhtar University, Libya.

E-*mail:* [1] ahmed.adil@omu.edu.ly ,[2] hakimawami. @gmail.com ,[3] Tarek.Hamad@omu.edu.ly .

**SPECIAL ISSUE ON:**

The 1st International Conference on Technical Sciences, 2024.
"Investing in Renewable Energies"
11 November 2024 SEBHA, LIBYA.

**KEYWORDS**

Photovoltaic, Mirror, Cell Temperature, Elbida.

**ABSTRACT**

The goal of this research is to provide an overview of a strategy for optimizing solar panel performance in the presence of solar tracking mirrors in order to optimize energy production. Under Elbieda's climatic conditions, as well as to investigate the fundamental effect of cell temperature on the performance of monocrystalline modules with a mirror reflector. According to the experimental results, the water-cooled concentrating PV system, the concentric PV system, and the solar panel had final plate temperatures of 56.2, 64.7, and 38.4°C, respectively. Furthermore, the panel receives an average of 47.73 watts, or about 56.15% of the panel's power, without the need of the inverter. When using an inverter (mirror), the panel produces an average power of 50.31 watts, accounting for 59.18% of its total power. The average power given to the panel by a water-cooled CPV system is 54.31 watts, or 63.89% of the panel's output. By using the mirror as a reflector and a water-cooled concentrating PV system, the system may create an extra 7.45% and 20.72% of electricity, respectively. In addition, using reflectors and water cooling with the PV panel increased power efficiency from 8.61% to 9.14%.

*Corresponding author.

DOI: https://doi.org/10.51646/jsesd.v14iFICTS-2024.443

# تحليل أداء الألواح الشمسية الكهروضوئية المعززة بعاكسات مستوية في البيضاء ليبيا: دراسة تجريبية

احمد عادل رشيد عثمان ، عبدالحكيم ابراهيم العوامي، طارق عبدالرحمن الترهوني.

**ملخص**: الغرض من هذه الدراسة هو تقديم مخطط لطريقة لتحسين أداء الألواح الشمسية في وجود مرايا تتبع الطاقة الشمسية من أجل تعظيم إنتاج الطاقة. في ظل الظروف المناخية لبيضاء، وكذلك لفحص التأثير الأساسي لدرجة حرارة الخلية على أداء الوحدات أحادية البلورة مع عاكس المرآة. وفقًا للنتائج التجريبية، كانت درجات حرارة اللوحة النهائية لنظام الطاقة الكهروضوئية المركزة المبردة بالماء، ونظام الطاقة الكهروضوئية المتحدة المركز، واللوحة الشمسية 56.2 و 64.7 و 38.4 درجة مئوية على التوالي. بالإضافة إلى ذلك، تتلقى اللوحة متوسط 47.73 واط، أي ما يقرب من 56.15٪ من طاقة اللوحة، دون استخدام العاكس. تحصل اللوحة على متوسط طاقة 50.31 واط عند استخدام العاكس (المرآة)، وهو ما يمثل 59.18٪ من طاقة اللوحة. يبلغ متوسط الطاقة التي يتم توصيلها إلى اللوحة عند استخدام نظام CPV المبرد بالماء 54.31 واط، أي ما يقرب من 63.89٪ من خرج اللوحة. من خلال استخدام المرآة كعاكس ونظام PV المركز المبرد بالماء، يكون النظام قادرًا على توليد 7.45٪ إضافية من الطاقة و 20.72٪ من الطاقة على التوالي. بالإضافة إلى ذلك، أدى استخدام العاكسات والتبريد بالماء مع لوحة PV إلى تحسين كفاءة الكهرباء من 8.61٪ إلى 9.14٪.

**الكلمات المفتاحية** – الطاقة الشمسية، المرآة، درجة حرارة الخلية،البيضاء.

## 1. INTRODUCTION

Renewable energy applications such as solar thermal energy, photovoltaics, geothermal energy, tidal power, wave power, wind power, hydropower, and biomass energy have already made major advances in the oil and gas industry globally. Libya has an area of 1,759,540 km ^2 and is located in North Africa, between 26 latitudes north and 17 longitudes east [1]. The Mediterranean Sea forms its northern border, followed by Egypt to the east, Sudan to the southeast, Algeria and Tunisia to the west, and Chad and Niger to the south. Libya's climate is affected by both the desert and the Mediterranean Sea.

Winter brings chilly temperatures and, on sometimes, rain to the coast. The Sahara is cold and dry in the winter and exceedingly dry and hot in the summer [1].

Over 80% of land is underutilized. Other than gathering solar energy, this land may not be used for agriculture or any other expected use [1]. Petroleum, natural gas, and fossil fuels have been Libya's primary sources of money, energy, industrialization, and prosperity for the past 20 years. Despite efforts to diversify revenue sources, fossil fuels continue to be critical to the nation's economy. Unfortunately, Figure 1 depicts how the fossil resources in this region are depleting. Complete reliance on gas and oil can have harmful consequences [2].

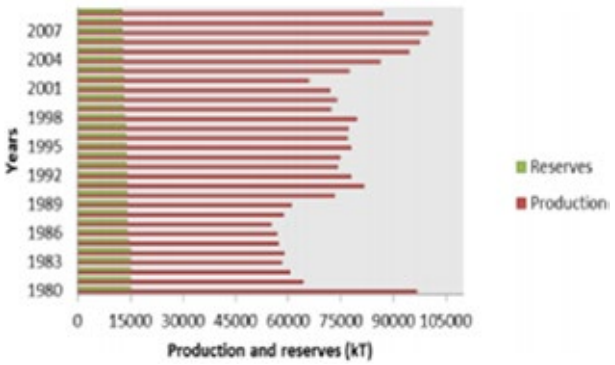


Figure 1. Libyan fossil fuel reserves and production versus time. [1,2].

" Libya relies entirely on fossil fuels to generate power, and the electricity generating sector is

regarded the most ecologically harmful, accounting for around 35% of total nation emissions [Source: Air pollution sources in Libya]. The Libyan government launched the Renewable Energy Strategic Plan for the next 30 years in response to the global trend of reducing pollution and mitigating the effects of global warming and climate change. The plan aims to achieve a 25% contribution of renewable energy to the electric energy mix by 2025 and 30% by 2030. Unlike now, by 2050, Libya will use more renewable energy than fossil energy. This will come primarily from solar energy [3].The sun is by far the largest energy source accessible on the planet: the amount of sun-oriented energy arriving to the earth's outer layer each year ( ) is multiple times greater than the global critical energy need and exceeds all available energy sources on the planet [4]. Furthermore, it is an endless and clean source of energy, which is critical in today's world: petroleum product assets are rapidly depleting, the population is growing, and environmental concerns are becoming increasingly real. The rapid conversion of this vast energy source into electrical energy with photovoltaic (PV) devices is likely the most potent and versatile approach for utilizing it. The first PV cells were developed in 1954 [4], and since then, technology has advanced, resulting in increased production and lower costs. The productivity of a standard level plate PV module, i.e., the capacity of a module to convert solar-powered energy into electrical energy, is still relatively low: while efficiencies of up to 25% have been achieved in research centers, efficiencies of only 14-17 % are still common in commercial use [4]. In any case, considering the Sun's vast quantity of energy, PV innovation's ability to create power remains outstanding. Cost has been the most major hindrance to the rapid expansion of PV displays thus far, as silicon, the most widely used material for PV modules, is expensive to produce. However, market development will typically reduce the costs of a unique innovation; for example, the PV innovation is now not extensively manufactured due to high prices, and cost reduction is impeded by the low level of production [5]. Nonetheless, improvements in both module technology and the assembly technique are continually lowering costs [6].Several factors determine the quantity of energy generated by a solar photovoltaic system [7]. Site-specific climatic parameters (solar insolation imposed on PV panel surfaces, wind speed, ambient temperature, and so on) as well as site-specific elements (latitude and longitude, dust and pollution levels, panel tilt angle, tracking design, installation height, rooftop type, shading, etc.). All of the aforementioned solutions will only work if they can reduce investment costs while increasing system efficiency. As a result, sun tracking techniques including single-axis, dual-axis, and mirror-augmented PV systems are more commonly used for large-scale energy extraction than other solar PV system approaches [8, 9]. Solar mirrors increase the amount of electricity generated by a given area of PV panels by collecting more direct sunlight on qualified PV modules [10]. Mirror Augmented Photovoltaics (MAPV) is a low concentration technique to collect more solar irradiation on a single PV panel. In our method, we use reflectors and PV systems. The mirror is less expensive, lighter, and scatters less light than a photovoltaic panel.

Figure 2. shows the experimental setup [12].

We can lower the cost of the balance of system (BOS) by producing more electricity from a single panel rather than adding more panels. [11] Figure 2 depicts Vincent Bourdin and Anne Migan-Dubois, who developed the Aleph experiment in 2011.

A variety of concentrator types are available to increase radiation flow to receivers. Both reflectors and refractors are options. They can be cylindrical or circular, depending whether you want to focus on a "line" or a "point." Concentrating collector systems include tubular absorbers with diffuse back reflectors, tubular absorbers with specular cusp reflectors, plane receivers with plane reflectors, parabolic concentrators, Fresnel reflectors, and heliostat arrays with a central receiver. Connecting one or more planar reflectors to the primary harvester system is the simplest and most cost-effective way to enhance the amount of solar energy that falls on the surface. Concentration devices can attain higher operating temperatures under clear sky conditions, but they require higher-quality optical components, more accurate production techniques, and a way to watch the sun in general. Adding a reflector to a collector, on the other hand, is the most effective way to use diffuse and beam (direct) radiation while maintaining a decent concentration and reducing tracking [13]. As shown in Figure 3, the first architecture comprises both a typical PV system and a mirror array structure.

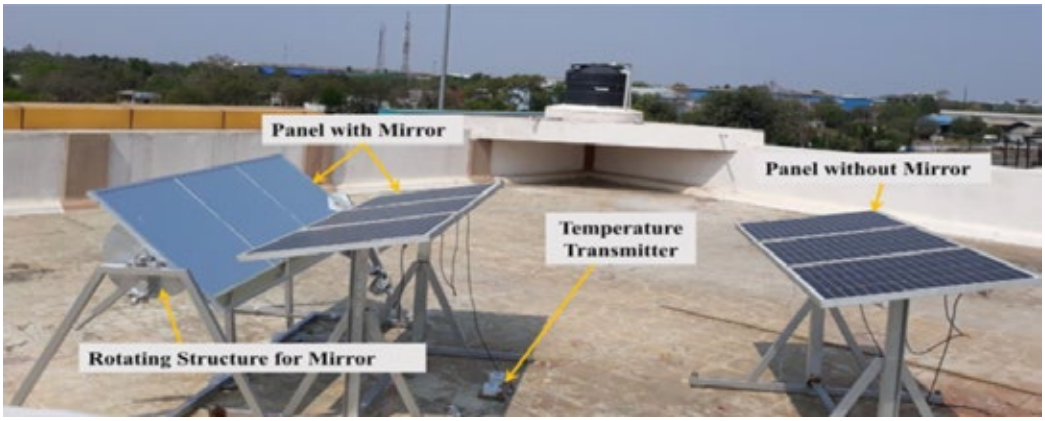


Figure 3. Demonstrates the experimental setup [14].

The plane reflector costs less than 5% of the PV system's cost, but it has the potential to boost solar energy collection by more than 15% per year within solar energy devices. As a result, plane reflectors appear to be a cost-effective technique to increase the efficiency of PV modules [15]. Using booster reflectors, on the other hand, has the potential to reduce the use of high-cost semiconductor materials, cutting the cost of manufacturing solar modules and producing electricity from photovoltaic systems.

It is well accepted that the output power of photovoltaic panels is proportional to the amount of incident solar radiation and the temperature of the photovoltaic cells. It is self-evident that increasing incidental solar radiation on a PV module produces more electricity. Using booster reflectors to improve the intensity of incidental irradiance on the PV panel surface is one proposed solution [16]. The primary goal of this research is to evaluate and assess the performance of regular PV modules, concentrated PV modules (CPV), and (CPV) systems using cooling techniques. Elbieda is a city in northeastern Libya.

The researcher will create a prototype to investigate, gather data, and analyze temperature distribution and air velocity.

Finally, the researcher will anticipate how much electricity can be produced.

## 2. METHODOLOGY

### 2.1. Experimental investigation

The study will be carried out in the Department of Mechanical Engineering at the University of Omar Al-Mokhtar's Faculty of Engineering in Elbida, Libya ( N; ° E).. Because the current study is focusing on the influence of the reflector on fixed PV systems, the solar module and reflector are installed at the optimal tilt angle for the site. Figure 4 depicts the experimental site.

Figure 4. El-Beida engineering faculty's experimental location.

Three monocrystalline photovoltaic modules (Type E850) with a peak power rating of will be used in this study's experimental setup to collect experimental data. The first unit is in regular operation and will serve as a reference, while the other units are Concentrated PV Units (CPV) and a CPV System with Cooling Technology. Under standard test circumstances of irradiation, cell temperature, and air mass, this module contains cells with short circuit current and open circuit voltage of and , respectively (AM). Table 1 provides more information regarding the PV module's specifications. Each solar panel in this study is equipped with one reflector. The reflector is 1.23 in length and 0.55 in width.

Table 1 Specifications of the PV module

| **Electrical Specification** | |
|---|---|
| **Model** | **TE850** |
| Peak power (***Pm***) | 85 W |
| Short circuit current (***Isc***) | 5.20 A |
| Open circuit voltage (***Voc***) | 22.0 V |
| Max. power current (***Im***) | 4.80 A |
| Max. Power voltage (***Vm***) | 18.1 V |
| Cell efficiency (%) | 15% |
| Mechanical Specification | |
| Dimensions (***L***x***W***x***D***) | 1231x556x24.5 |
| Weight | 7.8 Kg |
| Module area | 0.684 |

It is put up in such a way that no shadows fall on the solar panel. This experiment uses a flat glass reflector. A monocrystalline (m-Si) PV module with and without a mirror reflector and cooling system A tank with a capacity of 1,500 litters was employed. Placed at a height greater than the top edge of the board, permanently fed with water, and connected with a tube perforated with 15 holes with a diameter of 1.5 mm, placed on the upper edge of one of the boards, so that the water flows freely over the board's surface and covers the entire board surface. Was intended to acquire

the experimental outcomes of this investigation, as shown in Figure 5.

Figure 5. Elbida's experimental setup for regular PV modules, concentrated PV modules (CPV), and (CPV) systems with cooling is seen in this photograph.

Measurements were taken on a clear day in July 2021, from a.m. to p.m., with the goal of assessing PV module performance. Experimental data was gathered every half hour. During the testing period, measurable factors such as slope irradiance, ambient temperature, cell temperature, voltage, current, and wind speed were crucial and must be thoroughly analyzed. A pyranometer (RK200-03) was used to determine the intensity of solar radiation at the same tilt angle as the PV module. Module current and voltage measurements are used to provide exact information about the PV module's power output. An anemometer was used to determine wind speed. To measure cell temperature, a thermocouple was put on the PV module's front surface using thermal tape. Another thermocouple was used to measure the ambient temperature. All data was collected using a data logger and a signal converter device. Figure 6 shows the arrangement of the experimental set-up with many instruments.

Figure 6. Experimental setup layout.

## 2.2. Mathematical Modeling

The total solar radiation on the PV surface with the tilted plane, angle b, is the sum of direct solar radiation traveling in a straight line from the sun to the earth's surface, diffuse solar radiation

scattered in the atmosphere and reaching the earth's surface, and ground-reflected radiation (Figure 7). In the case of a flat reflector system, the direct and diffuse irradiances that strike the mirror's surface and are reflected on the PV module will be added (Figure 7). For the objectives of this study, a MATLAB software was used to construct a PV module model, which uses solar radiation and the ambient temperature of the site to estimate:

- The irradiance of a reflector-equipped panel.
- Increased irradiance affects the panel's temperature.
- The expected electrical output.

For the study, a one-hour time step was used. The monthly insolation data were used to create hourly solar radiation data using the procedures described in [17].

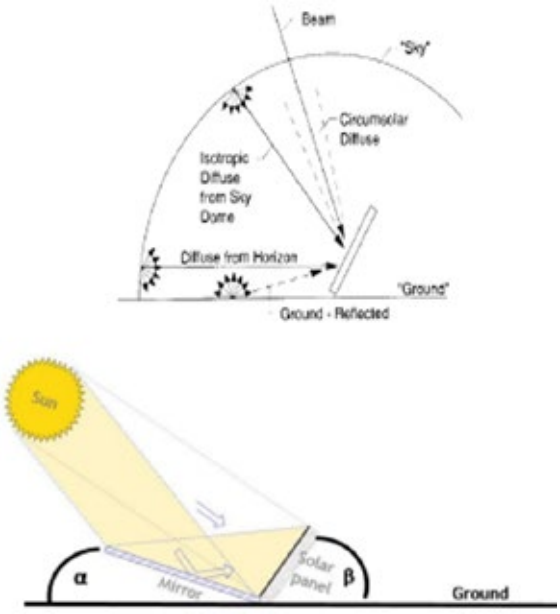


Figure 7. (a) Irradiances of a conventional PV system; and (b) a PV-reflector system [17].

### 2.2.1. Photovoltaic Irradiation model for the PV system with a mirror reflector

The total amount of solar energy from the sky (beam and diffuse), the ground (reflected), and the reflector equals the irradiance on the PV panel (spectral and diffuse). The irradiance on a slanted surface is analyzed in terms of direct (beam $H_B$), diffuse from the sky ($H_D$), and reflected from the ground ($H_R$), which are given by the following equations [17]:

$$H_T = H_B + H_D + H_R \qquad (1)$$

The beam irradiance at the slanted surface can be stated in ($H_B$):

$$H_B = (H_g + H_d)H_b \qquad (2)$$

$H_g$ and $H_d$ represent global and diffuse radiation on a horizontal surface. $H_b$ is the ratio of average daily beam radiation on a slanted surface to a level surface.

$$R_b = \frac{cos(\phi - \beta)cos\,\delta\,sin\,\omega + \omega_{rad}\,sin(\phi - \beta)sin\,\delta}{cos\,\phi\,cos\,\delta\,sin\,\delta + \omega_{rad}\,sin\,\phi\,sin\,\delta} \qquad (3)$$

Where β,ϕ,δ and ω are the tilt angle, latitude of the site, declination angle (δ) and the hour angle (ω) respectively.

- **Declination angle (δ):**

$$\delta = 23.45\,sin\left[360\left[\frac{284+n}{365}\right]\right] \qquad (4)$$

Where is number of days starting from 1st of January to the given date.

- **Hour angle (ω):**

$$\omega = cos^{-1}(-tan\,\delta\, tan(\phi - \beta)), \quad where \quad sin\,\delta = sin\,\phi \tag{5}$$

$$\omega = cos^{-1}(-tan\,\delta\, tan\,\phi), \quad where \quad sin\,\delta \neq sin\,\phi \tag{6}$$

$$and, \qquad sin\,(x) = \frac{x}{|x|}$$

The Diffuse radiation incident on a Tilted Surface ($H_D$):

$$H_D = R_d H_d \tag{7}$$

$R_D$ is the ratio of average daily diffuse radiation on a tilted surface to that on a level surface, calculated using the distribution of sky diffuse radiation over the globe. Assuming sky diffuse radiation is isotropic, $R_d$ may be determined using the following formula:

$$R_d = \frac{1 + cos\,\beta}{2} \tag{8}$$

Reflected radiation on a tilted surface ($H_R$): Reflected radiation without any reflectors surrounding the solar panels:

$$H_{R\ Ground} = H_g \rho \left( \frac{1 - cos\,\beta}{2} \right) \tag{9}$$

Where $\rho$ is the solar reflectivity of ground.

Considering all the elements described above, the goal function (Incident total radiation on slanted surface) may be represented as, without any reflectors.

$$H_{T\ Ground} = (H_g - H_d) R_d + H_d \left( \frac{1 + cos\,\beta}{2} \right) + H_g \rho \left( \frac{1 - cos\,\beta}{2} \right) \tag{10}$$

The solar panel's configuration a solar panel can be upgraded with the addition of mirror to boost energy output from a standard solar power plant, as illustrated in Figure 7.

(Total irradiance ($H_T$) =

[Beam irradiance + diffused irradiance + irradiance from ground reflection + irradiance from mirror reflection]).

$$H_T = (H_g - H_d) R_d + H_d \left( \frac{1 + cos\,\beta}{2} \right) + H_g \rho \left( \frac{1 - cos\,\beta}{2} \right) + R_{d,mirror} \rho_m \left( \frac{1 - cos(\alpha - \beta)}{2} \right) \tag{11}$$

Where $\rho_m$ is the solar reflectivity of mirror, and $R_{d,mirror}$ is the ratio of radiation on tilted surface to a horizontal surface.

$$R_{d,mirror} = \frac{1 + cos\,\alpha}{2} \tag{12}$$

### 2.2.2. Effect of temperature

According to the relationship [18], The real power ($P_{PV}$) of the PV panel under real operation and climatic conditions (solar radiation $H_t$ and ambient air temperature $T_\infty$ ) is calculated:

$$P_{PV} = P_{STC} \left[ 1 + \beta_p (T_{cell} - T_{STC}) \right] \frac{H_T}{H_{STC}} \tag{13}$$

Where: $T_{STC}$ and $T_{cell}$ are the celll's surface temperature at Standard Test Condition, $\beta_p$ is the power temperature coefficient.

The cell surface temperature $T_{cell}$ can be determined from [19]:

$$T_{cell} = T_{\infty} + 7.8\times10^{-2} H_T \qquad (14)$$

## 3. RESULT-AND DISCUSSION

A series of experiments were carried out to demonstrate the behavior of the standard PV module, concentrated PV module (CPV), and (CPV) system with cooling technology under El-Bieda climatic conditions. The tests and measurements include the following:

- Determine total irradiation on PV modules by measuring solar radiation intensity without a mirror reflector.
- Determine the solar radiation intensity for a PV system with a mirror reflector, including direct and reflected irradiation from the reflector and cooling (CPV).
- The temperature distribution for PV systems with and without mirror reflectors, as well as CPV systems with cooling.
- Air speed (ambient).
- Atmospheric temperature.

This section describes and assesses the experimental results. On July 25, 2021, the test will be carried out on a sunny day. The readings are taken between 8:00 a.m. and 5:00 p.m. On the day of the experiment, when the outside temperature ranged from 25 to 36 degrees Celsius, the solar radiation without (cpv) was 968 , whereas the solar radiation with (cpv) was 1128 .
According to the findings, as shown in Figure 10, water cooling has a substantial effect on the panel's temperature. The average panel temperature of the water-cooled CPV system was 34.3 , whereas the conventional PV panel and the CPV system had average panel temperatures of 64.7 and 56.2 , respectively. The water-cooling system reduced the CPV system's panel temperature by an average of 26.3 Figures 8, 9, 10, and 11 show the greatest power outputs of the water-cooled CPV system, conventional PV module, and CPV system, which were 54.3, 47.3, and 50.31 , respectively.

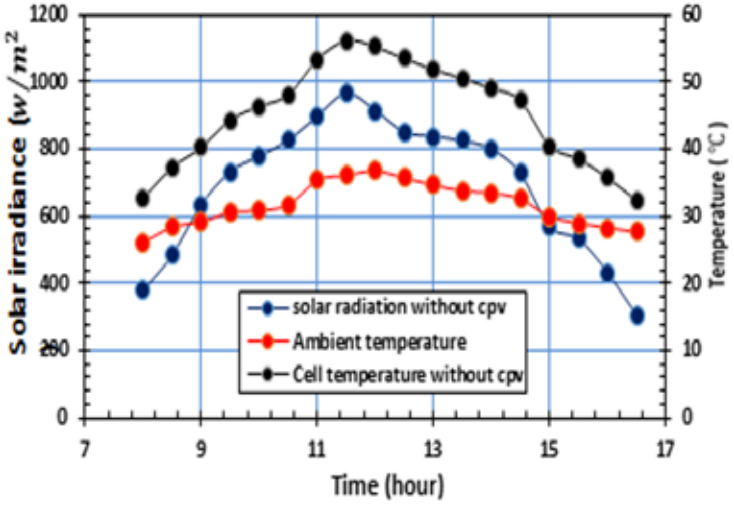


Figure 8. The PV module's test day saw changes in the ambient temperature, cell temperature, and slope irradiance.

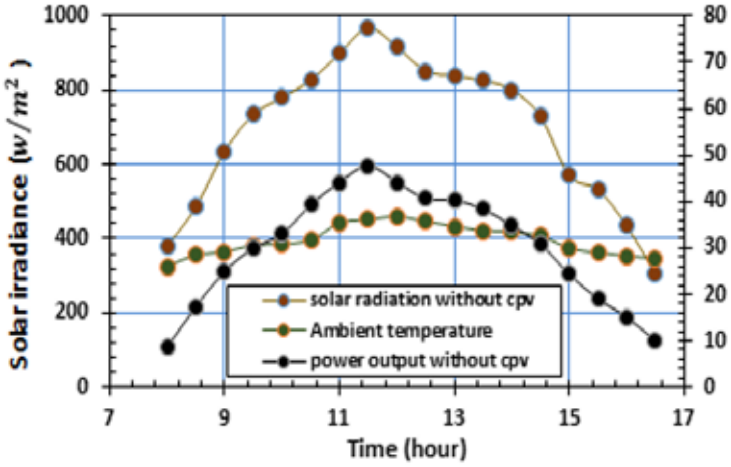


Figure 9. Change in slope irradiance and power production of the PV module on the best test day.

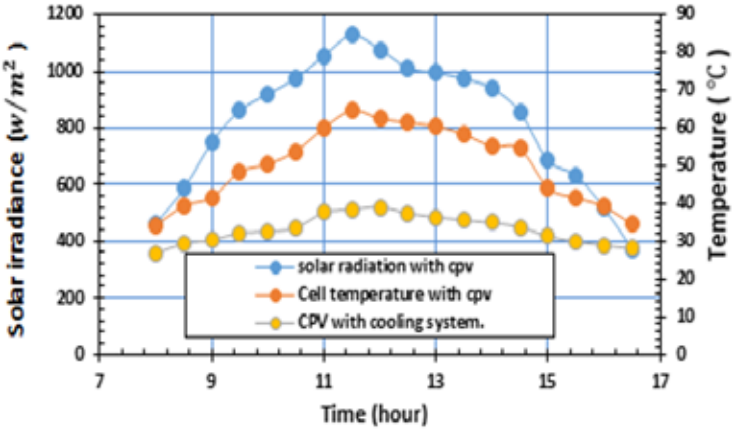


Figure 10. Changes in ambient temperature, cell temperature, and slope irradiance on the optimum test day for the PV with mirror and cooling system.

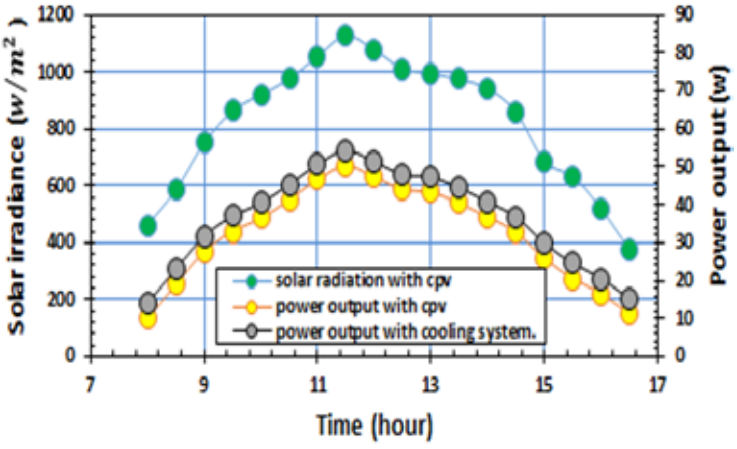


Figure 11. Change of slope irradiance and power production during the optimum test day for the PV with mirror and cooling system.

As is widely known, the efficiency of PV modules decreases as the temperature of the panels rises. This affects overall solar power plant power generation, particularly in hot climes, and other factors such as dust collection and PV deterioration also influence PV efficiency, necessitating corrective actions such as PV cooling and cleaning. However, in this portion of the Elbida region, the temperature effect on PV modules has not been demonstrated to be highly mi Weather conditions at the place (temperature, wind speed, humidity, etc.), reflector material, and so on. Rising solar cell temperatures will have an influence on PV efficiency. Because the temperature increase induced by the reflector is minor, the impact on PV efficiency is unlikely to be substantial in this investigation. Figure 12 shows that the highest electrical efficiency of the CPV system and the CPV with the cooling system are 8.87% and 9.14%, respectively, while the reference PV module efficiency is 8.61%. Furthermore, the performance ratios of the CPV system and the CPV with the cooling system improve by 59.18% and 63.89%, respectively. As depicted in Figure 13.

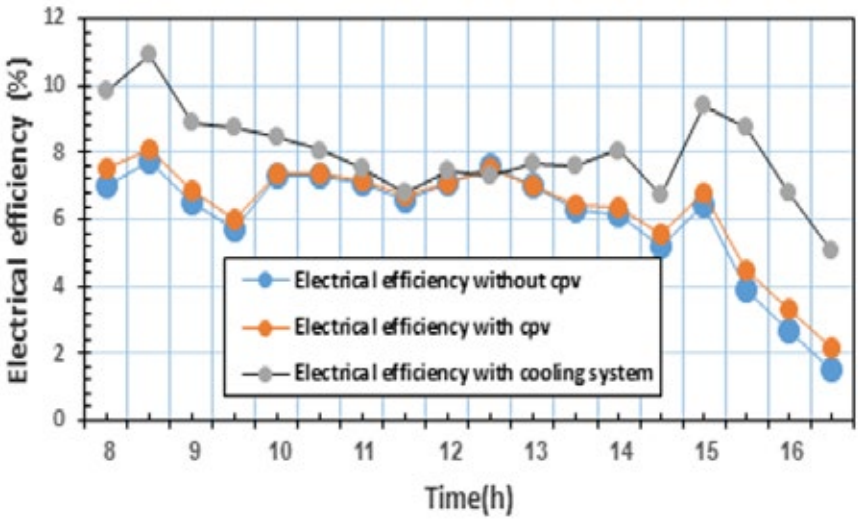


Figure 12. Changes in anticipated electrical efficiency for each system during the test day.

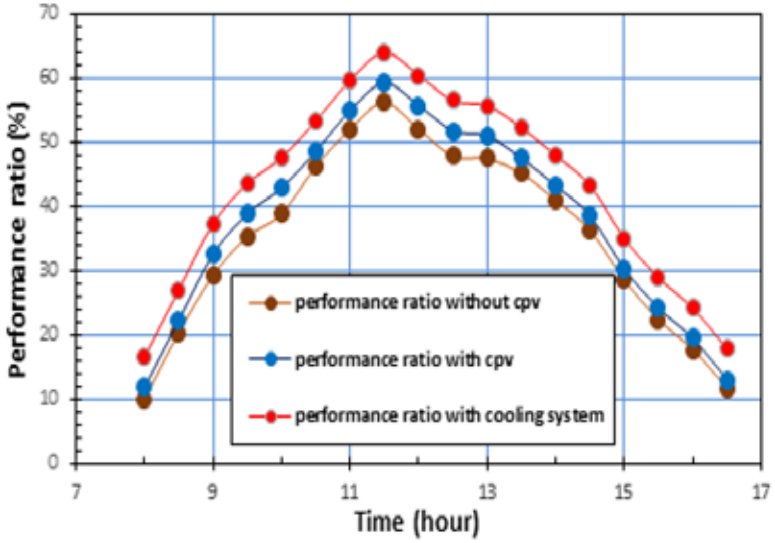


Figure 13. Differences in the expected performance ratio for each system during the test day.

Figures 14, 15 show the experimental I-V characteristic data across various time periods. Figures 13 and 14 demonstrate that using water cooling and reflectors increased the maximum open circuit voltage (V_OC) by about 11.11% while increasing the maximum short circuit current

(I_SC) by 3%. When using just reflectors, the maximum short circuit current increased by 8.1% and the maximum open circuit voltage decreased by 1.07%.

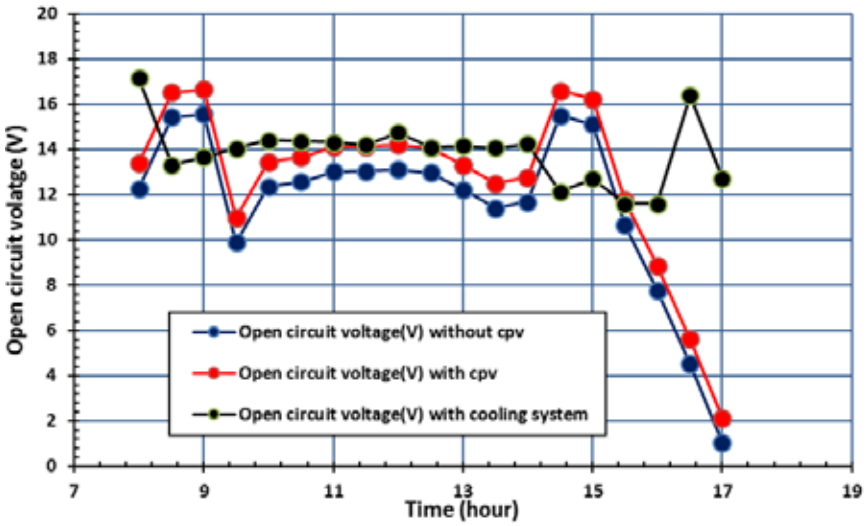


Figure 14. During the test day, the projected open circuit voltage (V) varied for each system.

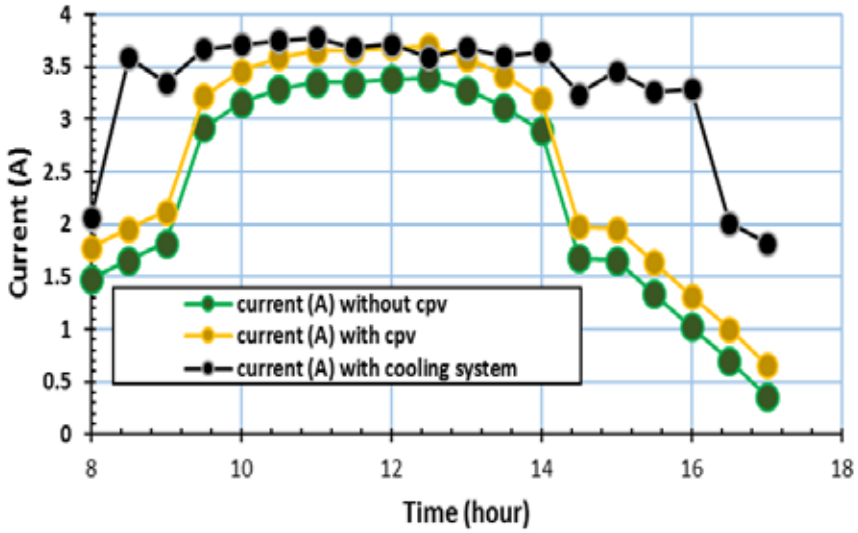


Figure 15. Changes in projected current (A) for each system on test day.

The changes of cell temperature and output power vs slope irradiance of the regular PV module, concentrated PV module (CPV), and (CPV) system with cooling throughout the test day are compared to those obtained from the PV module in order to evaluate PV performance. Figures 16, 17, and 18 demonstrate this idea clearly. These figures illustrate that cell temperature and output power are significantly impacted by slope irradiance circumstances. Cell temperature and output power increase with the slope irradiance level increases. Furthermore, around 11:30, the PV module's maximum cell temperature hits (56.2 ), yielding the highest slope irradiance value (968 ). In contrast, the concentrated PV module with (CPV) has a maximum cell temperature of just 64.7 . It is also worth mentioning that the maximum output power for PV with a (CPV) system with cooling system is (54.31 ), which is more than that of the PV module. The 5.42% increase in output power for the PV with plane mirror reflector system is substantial. The PV with plane mirror reflector system is important.

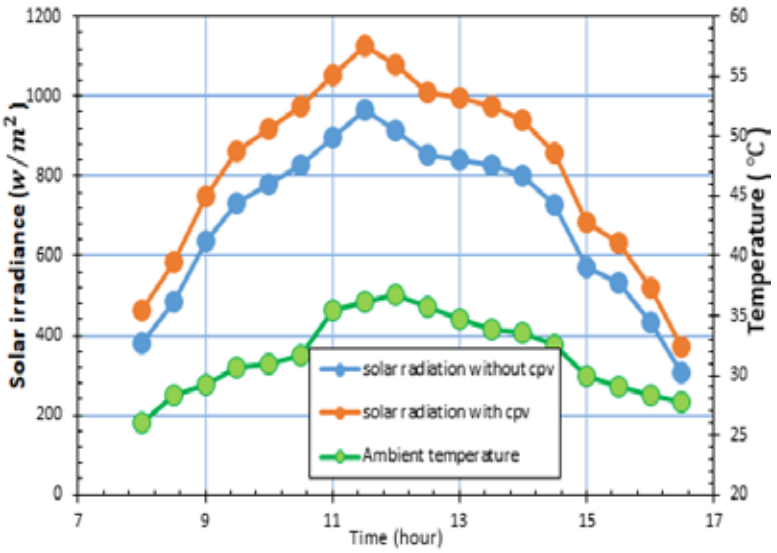


Figure 16. The reported slope irradiance and ambient temperature fluctuated during the day.

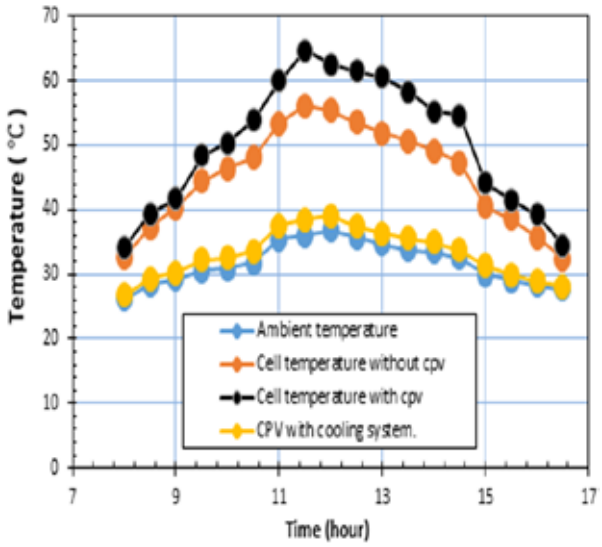


Figure 17. The reported cell temperature fluctuated during the day.

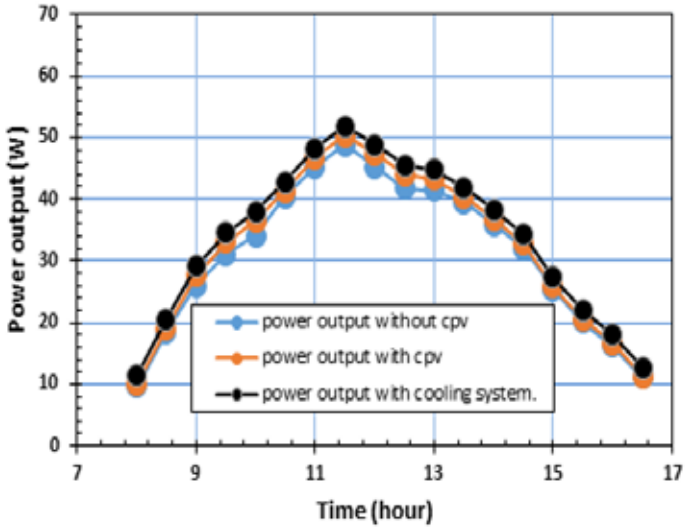


Figure 18. The power output varied during the day.

### 3.1. Model Validation

Experimental data was utilized to validate the estimated values of slope irradiance (PV with mirror), cell temperature (PV with mirror), and solar cell temperature from the built model. Furthermore, the slope irradiance was confirmed using data collected under various weather conditions. To accomplish so, well-known statistical markers are utilized to assess the correctness of calculated and experimental data. These metrics ($R^2$) are calculated using the mean bias error (MBE), root mean square error (RMSE), and coefficient of determination equations.

$$MAE = \frac{\sum_{i=1}^{N} |y_i - \hat{y}_i|}{N} \quad (15)$$

$$MAPE = \frac{\sum_{i=1}^{N} |y_i - \hat{y}_i|}{N} \times 100\% \quad (16)$$

$$RMSE = \sqrt{\frac{\sum_{i=1}^{N} (y_i - \hat{y}_i)^2}{N}} \quad (17)$$

Smaller *RMSE* numbers indicate that the forecast was more accurate than the measured value.

$$R = \frac{\sum_{i=1}^{N} (y_i - \bar{y})(\hat{y}_i - \bar{\hat{y}})}{\sqrt{\sum_{i=1}^{N} (y_i - \bar{y})^2 \sum_{i=1}^{N} (\hat{y}_i - \bar{\hat{y}})^2}} \quad (18)$$

In the range $-1 \le R \le 1$ , the correlation coefficient is defined as:

- If $R=-1$ is true, $y_i$ and $\hat{y}_i$ have an ideal negative linear relationship.
- If $R=1$ is true, $y_i$ and $\hat{y}_i$ have a completely positive linear relationship.
- If $R=0$ is true, $y_i$ and $\hat{y}_i$ do not form a linear link.

Where ( $y_i$ , $\hat{y}_i$ , $\bar{y}$ ) and ( $\bar{\hat{y}}$ ) represent its calculated value, measured value, calculated value average, and measured value average, respectively [20].

Solar irradiance data was measured and converted to slope irradiance, as specified in section and was recorded from sunrise to sunset, with a focus on the test day. The projected slope irradiance is then compared to the observed sloping surface irradiance.

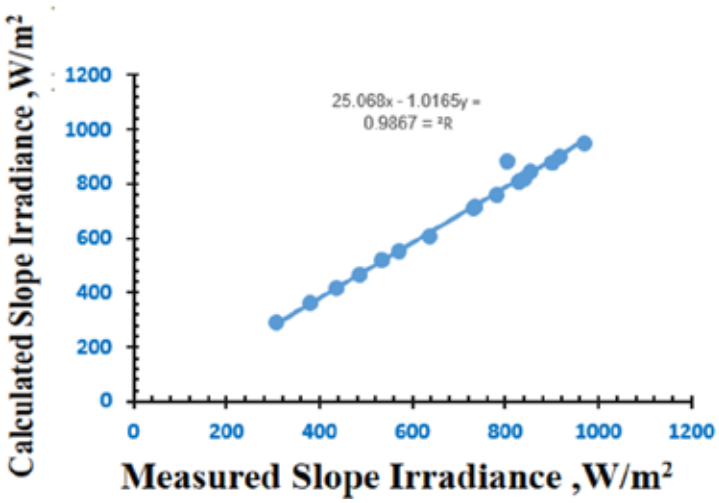


Figure 19. Compare the results of an experiment with a slope irradiance estimate during the test period.

Theoretical and experimental data can be compared by putting them on the same graph and comparing the results. The line 1:1 (slope equal to 1 and y-interception equal to 0) should be the result if the anticipated values exactly match the data.

Figure 19 shows a comparison of observed slope irradiance to that calculated using the MATLAB technique. The graph shows the coefficient of determination ($R^2$), mean bias error (MBE), and root mean square error (RMSE) as 0.987, -13.611, and 26.774, respectively. These values are deemed substantial, making them more likely to be dependable. As can be seen, the determined slope of the correlation between observed and calculated slope irradiance is similarly 0.964. The slope irradiance percentage relative error is then calculated to be 16.7%. (Using measured data as a reference). The slope irradiance varies by 3.6% from what is projected.

Figures 20 and 21 compare the simulated and experimental findings. The coefficient of determination (R^2), mean bias error (MBE), and root mean square error (RMSE) for cell temperature are 0.97, -0.637, and 1.751, respectively, and for slope irradiance (PV with mirror) are 0.989, 27.444, and 36.913, respectively, which are primarily considered to be significant and more likely reliable. Figure 20 depicts the slope of the relationship between observed and estimated cell temperature, which was determined to be 0.9884. The slope of the observed-to-computed Slope irradiance for PV with mirror. It was determined to be 0.948, as seen in the figure 21.

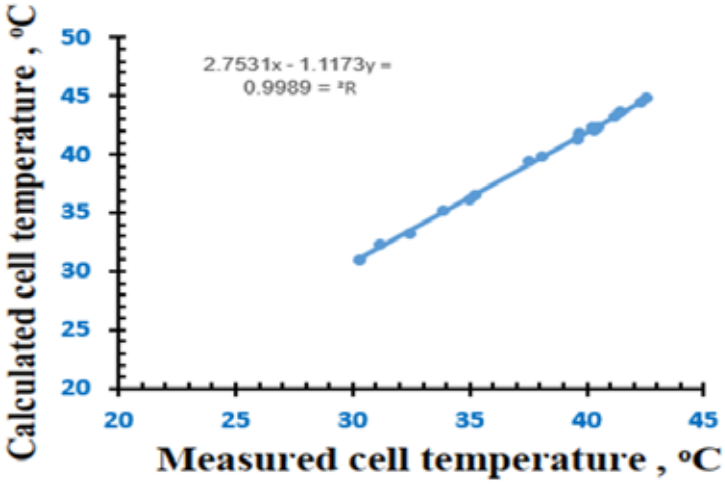


Figure 20. Experiment compared to calculating cell temperature during the test time.

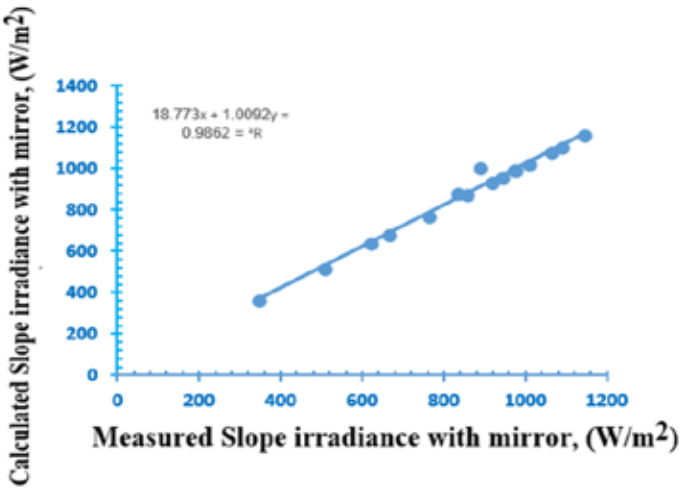


Figure 21. Experiment compared. computation of slope irradiance with mirror during the test period.

To determine the % relative to the measured data, divide the percentage relative to the measured data by the percentage relative to the measured data. For (PV with mirror), errors in cell

temperature and slope irradiance are calculated and estimated to be the slope irradiance for PV (with mirror). Should be 2.04%, and cell temperature should be 2.93%. The slope irradiance for PV with a mirror differs by 0.7% from the expected cell temperature value, although there is a 1% discrepancy.

## 4. CONCLUSIONS

The primary goal of this research is to assess the performance of a conventional PV module, concentrated PV module (CPV), and (CPV) system with cooling, both theoretically and practically. The current inquiry led to the following conclusions:

- The energy laboratory at the Elbida Faculty of Engineering was used to conduct outside testing on the target designs of regular PV modules, concentrated PV modules (CPV), and CPV systems with cooling.
- In the future, it will be a more cost-effective and efficient energy source. However, this technology's core cost remains greater than nuclear, thermal, or wind generation. Combining reflectors with PV panels to capture more light from the modules is a simple and practical technique to cut PV power expenses. Using an ideal design configuration, the performance of a conventional PV module, concentrated PV module (CPV), and (CPV) system with cooling was tested.
- The following measurements were taken: cell temperature, slope irradiance, ambient temperature, wind speed, voltage, and current.
- The cooling system effectively reduced the panel's temperature by 26.3 .
- The water-cooled CPV system and the CPV system have greater maximum power outputs, 20.72% and 7.45%, respectively.
- Using a water cooling system with solar concentration resulted in a maximum electricity efficiency of 9.14%, whereas a standard PV panel achieved 8.87%.
- When appropriate information was supplied to compare the recommended configuration with reviewed literature in terms of boosting power generation and reducing panel temperature, it was feasible compared to previous studies.
- Research shows that using bottom reflectors in a PV system increases power output capacity. In the case of big power plants, this would result in greater land utilization efficiency and fewer PV panels, lowering installation and land costs while increasing revenue from the power plant's energy production. This functionality requires more investigation.
- The current study focuses on non-tracking PV system power increase utilizing mirror reflectors. However, the recommended model may also be used with manual/automatic tracking of reflectors fixed at the ideal tilt angle for optimal power generation throughout the year. Follow-up research using single and double axis PV and reflector tracking systems can be conducted in cold and hot

**Authors contribution:** All authors have made a substantial, direct, and intellectual contribution to the work and approved it for publication.
**Funding:** There is no funding for the article.
**Data Availability Statement:** Not applicable.
**Conflicts of Interest:** The authors declare that there is no conflict of interest.

## REFERENCES

[1] Hamad, T. A. M. (2015). System integration of hydrogen energy technologies using renewable energy resources. Missouri University of Science and Technology.

[2] Belkhair, A., & Hamad, T. (2019, March). Estimating the Amount of Methane Gas Generated from the Feedstock: A Case Study of El-Beida City, Libya. In 2019 10th International Renewable Energy Congress (IREC) (pp. 1-5). IEEE.

[3] Nassar, Y., Alatrash, A., Elzer, R., Alkhazmi, A., El-Khozondar, H., Alsharif, A., ... & Khaleel, M. (2024). Optimum number of glass covers of thermal flat plate solar collectors. Wadi Alshatti University Journal of Pure and Applied Sciences, 2(1), 1-10

[4] Quaschning, V. (2005). Understanding Renewable Energy Systems: Earthscan. ISBN.

[5] Sandén, B. A. (2005). The economic and institutional rationale of PV subsidies. Solar energy, 78(2), 137-146.

[6] Swanson, R. M. (2006). A vision for crystalline silicon photovoltaics. Progress in photovoltaics: Research and Applications, 14(5), 443-453.

[7] Hosenuzzaman, M., Rahim, N. A., Selvaraj, J., & Hasanuzzaman, M. (2014, November). Factors affecting the PV based power generation. In 3rd IET International Conference on Clean Energy and Technology (CEAT) 2014 (pp. 1-6). IET.

[8] Dolara, A., Grimaccia, F., Leva, S., Mussetta, M., Faranda, R., & Gualdoni, M. (2012). Performance analysis of a single-axis tracking PV system. IEEE Journal of Photovoltaics, 2(4), 524-531.

[9] Pelaez, S. A., Deline, C., Greenberg, P., Stein, J. S., & Kostuk, R. K. (2019). Model and validation of single-axis tracking with bifacial PV. IEEE Journal of Photovoltaics, 9(3), 715-721.

[10] French, R. H., Murray, M. P., Lin, W. C., Shell, K. A., Brown, S. A., Schuetz, M. A., & Davis, R. J. (2011, May). Solar radiation durability of materials components and systems for low concentration photovoltaic systems. In IEEE 2011 EnergyTech (pp. 1-5). IEEE.

[11] Lin, W. C., Hollingshead, D., French, R. H., Shell, K. A., Schuetz, M., & Karas, J. (2012, June). Non-tracked mirror-augmented photovoltaic design and performance. In 2012 38th IEEE Photovoltaic Specialists Conference (pp. 002076-002081). IEEE.

[12] Baccoli, R., Mastino, C. C., Innamorati, R., Serra, L., Curreli, S., Ghiani, E., & Marini, M. (2015). A mathematical model of a solar collector augmented by a flat plate above reflector: Optimum inclination of collector and reflector. Energy Procedia, 81, 205-214.

[13] Pavlov, M. (2016). Numerical modelling of the coupling of thermal and photoelectric effects for the photovoltaic modules under low concentration (Doctoral dissertation, Université Paris-Saclay).

[14] Simon, S. P., Kumar, K. A., Sundareswaran, K., Nayak, P. S. R., & Padhy, N. P. (2020). Impact and economic assessment on solar PV mirroring system–A feasibility report. Energy Conversion and Management, 203, 112222.

[15] Ahmad, G. E., & Hussein, H. M. S. (2001). Comparative study of PV modules with and without a tilted plane reflector. Energy conversion and management, 42(11), 1327-1333.

[16] Tabaei, H., & Ameri, M. (2015). Improving the effectiveness of a photovoltaic water pumping system by using booster reflector and cooling array surface by a film of water. Iranian Journal of Science and Technology Transactions of Mechanical Engineering, 39(M1), 51-60.

[17] Vidanalage, I., & Raahemifar, K. (2016, October). Tilt angle optimization for maximum solar

*power generation of a solar power plant with mirrors. In 2016 IEEE electrical power and energy conference (EPEC) (pp. 1-5). IEEE.*

*[18] Hafez, A. A., Nassar, Y. F., Hammdan, M. I., & Alsadi, S. Y. (2020). Technical and economic feasibility of utility-scale solar energy conversion systems in Saudi Arabia. Iranian Journal of Science and Technology, Transactions of Electrical Engineering, 44, 213-225.*

*[19] Nassar, Y. F., & Salem, A. A. (2007). The reliability of the photovoltaic utilization in southern cities of Libya. Desalination, 209(1-3), 86-90.*

*[20] Sarhaddi, F., Farahat, S., Ajam, H., & Behzadmehr, A. (2010). Exergetic performance assessment of a solar photovoltaic thermal (PV/T) air collector. Energy and Buildings, 42(11), 2184-2199.*